Published in final edited form as:
Cancer Res. 2014 June 1; 74(11): 2962–2973. doi:10.1158/0008-5472.CAN-13-2421.

Myeloid WNT7b mediates the angiogenic switch and metastasis in breast cancer

Eun-Jin Yeo[1,2,#], **Luca Cassetta**[3,#], **Bin-Zhi Qian**[3,#], **Ian Lewkowich**[4], **Jiu-feng Li**[3], **James A. Stefater III**[1,2], **April N. Smith**[1,2], **Lisa S. Wiechmann**[5], **Yihong Wang**[6], **Jeffrey W. Pollard**[3,*], and **Richard A. Lang**[1,2,*]

[1]The Visual Systems Group, Divisions of Pediatric Ophthalmology and Developmental Biology, Cincinnati Children's Hospital Medical Center, Cincinnati, OH 45229, USA

[2]Department of Ophthalmology, University of Cincinnati, Cincinnati, OH 45229, USA

[3]Department of Developmental and Molecular Biology, Albert Einstein Cancer Center, Albert Einstein College of Medicine, Bronx, NY 10461, USA

[4]Division of Immunobiology, Cincinnati Children's Hospital Medical Center, Cincinnati, OH 45229, USA

[5]Department of Surgery, Albert Einstein Cancer Center, Albert Einstein College of Medicine, Bronx, NY 10461, USA

[6]Department of Pathology, Albert Einstein Cancer Center, Albert Einstein College of Medicine, Bronx, NY 10461, USA

[7]Department of Obstetrics and Gynecology and Women's Health, Albert Einstein Cancer Center, Albert Einstein College of Medicine, Bronx, NY 10461, USA

Abstract

Oncogenic targets acting in both tumor cells and tumor stromal cells may offer special therapeutic appeal. Interrogation of the Oncomine database revealed that 52/53 human breast carcinomas showed substantial upregulation WNT family ligand WNT7B. Immunolabeling of human mammary carcinoma showed that WNT7B immunoreactivity was associated with both tumor cells and with tumor associated macrophages (TAMs). In the MMTV-PymT mouse model of mammary carcinoma, we found tumor progression relied upon Wnt7b produced by myeloid cells in the microenvironment. Wnt7b deletion in myeloid cells reduced the mass and volume of tumors due to a failure in the angiogenic switch. In the tumor overall, there was no change in expression of Wnt/β-catenin pathway target genes, but in vascular endothelial cells (VEC) expression of these genes was reduced suggesting that VEC respond to Wnt/β-catenin signaling. Mechanistic

[*]Corresponding authors: **Richard A. Lang**, Division of Pediatric Ophthalmology, Cincinnati Children's Hospital Medical Center, 3333 Burnet Avenue, Cincinnati, OH 45229, USA. Tel: 513-636-2700 (Office), 513-803-2230 (Assistant), Fax: 513-636-4317. Richard.Lang@cchmc.org, **Jeffrey W. Pollard**, Department of Developmental and Molecular Biology, Albert Einstein Cancer Center, Albert Einstein College of Medicine, 1300 Morris Park Avenue, Bronx, NY 10461, USA. Tel: (718) 430-2090, Fax: (718) 430-8972, jeffrey.pollard@einstein.yu.edu and Director, MRC Center for Reproductive Health, Queen's Medical Research Institute, 47 Little France Crescent, Edinburgh, EH16 4TJ, UK jeff.pollard@ed.ac.uk.
[#]E-J Y, LC and B-ZQ contributed equally to this research

Conflicts of Interest: There are no conflicts of interest.

investigations revealed that failure of the angiogenic switch could be attributed to reduced Vegfa mRNA and protein expression in VECs, a source of Vegfa mRNA in the tumor which was limiting in the absence of myeloid Wnt7b. We also noted a dramatic reduction in lung metastasis associated with decreased macrophage-mediated tumor cell invasion. Together these results illustrated the critical role of myeloid Wnt7b in tumor progression, acting at the levels of angiogenesis, invasion and metastasis. We suggest that therapeutic suppression of Wnt7b signaling might be advantageous due to targeting multiple aspects of tumor progression.

Keywords

Wnt7b; macrophage; myeloid; tumor angiogenesis; tumor metastasis

Introduction

Emerging evidence has shown that in mammary carcinoma, hematopoietic cells recruited to the tumor stroma contribute to tumor progression and metastasis (1, 2). Of these cells, extensive evidence shows that tumor-associated macrophages (TAMs) contribute to tumor progression and malignancy (3). These TAM actions are multi-factorial with individual populations having pro-tumoral properties including remodeling extracellular matrix, stimulating angiogenesis, and promoting tumor cell intravasation and extravasation as well as persistent growth at the metastatic site (4–6). In the primary tumor TAMs promote the dramatic increase in vascular density known as the angiogenic switch that is a rate limiting step for the transition of benign tumors to invasive carcinomas. The TAM population expresses Tie2 and its ablation results in inhibition of angiogenesis in a wide range of cancer models (7, 8). There is also a dynamic interplay of TAMs with cells of the acquired immune system (9). In mammary tumors these TAMs are regulated by $CD4^+$ T cells through their synthesis of IL-4 or IL-17 (10, 11). This cytokine signaling enhances their promotion of tumor cell invasion and metastasis but not their pro-angiogenic properties (10).

The WNT/β-catenin pathway has a critical role in normal development and tumorigenesis (12). Stabilizing exon 3 mutations in *CTNNB1*, low membrane β-catenin expression or its nuclear localization are significantly associated with poor cancer prognosis (13, 14). Abnormal expression of APC, a negative regulator of β-catenin, is also a major cause of colon cancer (15, 16). Furthermore, the gene for Axin, another negative regulator of the WNT/β-catenin pathway, is deleted in many types of cancer (17, 18). The suggestion that WNT ligands may be involved in mammary tumor progression comes from mouse mammary tumor virus (MMTV) insertional activation of the *Wnt1* gene (19), the observation that the ligands are expressed in human cancers (20, 21) and the demonstration that Wnt co-receptor Lrp5-deficient mice are resistant to Wnt1-induced mammary tumors (22). Recently, it has been reported that invasive TAMs from the mouse model of breast cancer caused by mammary expression of the Polyoma Middle T oncoprotein (MMTV-PyMT) express several Wnt genes, especially *Wnt5b* and *Wnt7b* (23). WNT7b has been implicated in prostate cancer (24) in modulation of vascularity during development (25, 26) and is significantly up-regulated in tumor-promoting TAMs (23, 27). To assess the function of this Wnt ligand in TAMs of the MMTV-PyMT model, we conditionally deleted *Wnt7b*

using the *Csf1r-icre* mouse line in which cre recombinase is expressed from the promoter for the Colony stimulating factor 1 receptor (28). This conditional ablation showed that in infiltrating myeloid cells Wnt7b is required for the angiogenic switch, tumor progression, tumor cell invasion and metastasis.

Materials and Methods

Mouse strains and Genotyping

All experiments were conducted in accordance with guidelines of Institutional Animal Care and Use Committee. Mouse lines used in this study include the *Wnt7b*^{tm2Amc} (29), *MMTV-PyMT* (30) and *Csf1r-icre* (28) lines and were genotyped according to published protocols.

Flow Cytometry

Human—Human ER+ breast cancers were taken from the clinic and minced finely with scissors and digested with enzyme solution (2 mg/ml collagenase A in 40 ml DMEM + 80 μl DNase (50 U/ml) for 1 hour at 37°C and filtered through a 70 μm nylon strainer. Single cells were stained for live/dead cells, regained and then incubated with antibodies as appropriate in the dark (Fig. S1). Human TAMs were isolated by flow cytometry using labeling for anti-CD45, anti-CD11b, anti-CD14 and anti-CD163. Analysis of human samples received approval by the Institutional Review Board of Albert Einstein College of Medicine.

Mouse—Tumors dissected from inguinal mammary glands free of the lymph node were minced, digested in Liberase (Sigma) and DNAse 1 reduced to single cell suspensions as described (31). Flow cytometry was performed using anti-CD3-PE (Clone 17A2), anti-B220-APC (Clone RA3-6B2), anti-mouse CD45-PE-Cy7 (Clone 30-F11), anti-F4/80-APC-eFluor 780 (Clone BM8), CD45 microbeads, anti-mouse CD31-APC (Clone 390), and anti-mouse CD105-PE (Clone MJ7/18). Macrophages were also labeled with fluorescent dextran via phagocytic uptake as previously described (32). Flow cytometric sorting of Endothelial cell with FACS Aria II (BD) was performed using anti CD45-APC (clone 30-F11) and anti CD31-PE-Cy7 (clone 390). Cells were collected in 1.5 ml tubes, centrifuged 10 min at 450 rcf and the pellet resuspended in cell lysis buffer. RNA extraction was performed using the Qiagen Micro Kit and retrotrascription performed with Superscript Vilo cDNA synthesis kit (Invitrogen).

Assessment of *Wnt7b* expression and *Wnt7b*^{tm2Amc} deletion in sorted cells

Flow sorted, tumor associated F4/80-positive macrophages, T cells, B cells and VECs were used for isolation of mRNA and genomic DNA. The primers used to assess expression of *Wnt7b* mRNA by RTPCR were; forward: 5'-ACGTGTTTCTCTGCTTTGGC-3', reverse: 5'-CCAGGCCAGGAATCTTGTT-3'. Control actin primers were; forward 5'-CGGTGCTAAGAAGGCTGTTC-3', reverse 5'-CTTCTCCATGTCGTCCCAGT-3'. Assessment of *Wnt7b*^{tm2Amc} deletion was performed as with the D3 forward and C3 reverse primers (33).

Histological analysis and volume quantification of mammary tumors

Tissue was fixed in 4% paraformaldehyde, processed and sectioned according to established procedures. For immunostaining, sections rehydrated and labeled using the TSA Detection kit (Invitrogen) and goat anti-PECAM antibody at 1: 100 dilution (M-20, Santa Cruz) or rabbit monoclonal Ki67 at 1:1000 (Neomarkers, RM-9106-S0). Functional blood vessels were identified using injected Texas red-conjugated Dextran according to established procedures (34). Gland volume was calculated as described (35).

RNA isolation and QPCR

RNA was extracted with TRIzol (Invitrogen) and used for quantitative PCR according to established procedures. The primers used were;

β-actin, fwd: 5'TTCTTTGCAGCTCCTTCGTT, reverse : 5'ATGGAGGGGAATACAGCCC,

Wn7b, fwd, 5'AGCTCGGAGCATTGTCATCC, rev, 5'TCACAATGATGGCATCGGGT

Dll4, : fwd, GGCATGCCTGGGAAGTATCC, rev, 5'GGCTTCTCACTGTGTAACCGA

Hey1, fwd, CGAGACCATCGAGGTGGAAA, rev, 5'CTCGATGATGCCTCTCCGTC

Vegfa, fwd : 5'GGAGATCCTTCGAGGAGCACTT, rev, 5'GGCGATTTAGCAGCAGATATAAGAA

Vegfr1, fwd, 5'GGCATCCCTCGGCCAACAATC, rev, 5'AGTTGCTGCTGGGATCCAGG

Vegfr2, fwd, 5'CGTTAAGCGGGCCAATGAAG, rev, 5'CTAGTTTCAGCCGGTCCCTG

Vegfr3, fwd, 5'CCGCAAGTGCATTCACAGAG, rev, 5'TCGGACATAGTCGGGGTCTT

Assessment of the pulmonary metastatic burden was performed using QPCR for the PyMT transcript. Lungs were removed before removing mammary glands to avoid cross contamination. The PyMT primers used were; forward: 5'-CTCCAACAGATACACCCGCACATACT-3', reverse: 5'-GCTGGTCTTGGTCGCTTTCTGGATAC-3'.

Immunoblotting

Immunoblotting using 50 μg of tumor cell lysate was carried out using standard methods. The antibodies used were rabbit anti-VEGF (A-20, Santa Cruz) and rabbit anti-β-tubulin (ab6046, Abcam).

In vivo invasion assay

Cell collection into needles placed in the primary tumor of anesthetized mice was carried out as described previously (36).

Statistical analysis

All statistical analyses were performed using SPSS for Windows version 18.0. Student's t test, Mann-Whitney U test and, for the frequency of tumor stage, Fisher's exact test was employed. A p value less than or equal to 0.05 was considered statistically significant.

Results

To determine whether WNT7B expression was associated with breast cancer in humans, we interrogated the Tissue Cancer Genome Atlas and Oncomine database (37). In the Finak et al data (38) set that independently performed expression analysis on tumor stroma, out of 53 mammary carcinomas, 52 showed significantly enhanced expression of *WNT7B* in the stroma and this was highly significant compared with normal breast (Fig. 1A, B). Furthermore, in a meta-analysis of recent gene expression profiling, increased *WNT7B* expression was significantly associated with breast carcinoma compared with normal (Fig. 1C). To determine directly whether TAMs from human breast cancers expressed *WNT7B*, we flow sorted macrophages from ER+ breast cancers using CD45+, CD11b+, CD14+, and CD163+ (Supplemental Fig. 1A–C) and performed RT-PCR for *WNT7B* (Fig. 1D). This analysis showed amplification products for *WNT7B* consistent with their significant over-expression in the stroma of breast cancer, while adjacent normal mammary tissue and that derived from reduction mammoplasty showed less expression. To assess the distribution of WNT7B protein in human breast cancers, we performed immunolabeling. Co-labeling with antibodies to WNT7B and for the TAM markers CD68 and CD163 showed that TAMs co-localized with WNT7B immunoreactivity (Fig. 1E–N). The most intense WNT7B immunoreactivity was in tumor cells (Fig. 1E). However, when regions of CD68 (Fig. 1E–G) and CD163 (Fig. 1H–N) labeling were magnified and the labeling channels separated, it was clear that WNT7B immunoreactivity was also found in TAMs. Most often, WNT7B immunoreactivity was associated with CD68 or CD163-labeled structures with the features of macrophage processes (Fig. 1F, G, I–K, M, N). On average, 61% of cells within the tumor were WNT7B immunoreactive. 15% of the total cells within the tumor were both myeloid (according to CD163 labeling) and immunoreactive for WNT7B. Combined, this data mining and direct expression assessment in human mammary tumors suggested that WNT7B produced by TAMs in the tumor stroma could play a role in tumor progression.

To analyze the role of macrophage-derived WNT7b experimentally in vivo, we generated conditional loss of function mice using the *Wnt7b*^{tm2Amc} allele (29) and the *Csf1r-icre* transgene (28) in the MMTV-PyMT model of mammary carcinoma (30). This tumor has most of the features of human mammary carcinoma, including ER positivity and progression through equivalent stages (30). This tumor also shows expression of Wnt7b in TAMs, particularly those TAMs that are invasive (23). Consistent with these data, RT-PCR on flow sorted F4/80+, dextran+ TAMs showed that these cells express *Wnt7b* in control *Wnt7b*$^{tm2Amc/-}$ mice (Fig. 2A). As expected, this expression is undetectable in TAMs from the conditional mutant, *Wnt7b*$^{-/tm2Amc}$*; Csf1r-icre* (Fig. 2A). Efficient deletion of the conditional *Wnt7b* allele was confirmed by DNA genotyping (Fig. 2B) of flow-sorted TAMs.

QPCR analysis also revealed that in the normal progression from hyperplasia/adenoma to early and late carcinoma in the MMTV-PyMT model, the expression level of *Wnt7b* transcripts increases (Fig. 2C, gray bars). By contrast, tumors from *Wnt7b*$^{-/tm2Amc}$*; Csf1r-icre* mice show a level of *Wnt7b* expression that does not increase significantly with tumor progression (Fig. 2C, blue bars). Deletion of *Wnt7b* from TAMs did not result in any statistically significant difference in the populations of recruited F4/80+ macrophages (Fig. 2D), CD3+ T cells (Fig. 2D), and B220+ B cells (Fig. 2D).

In several mouse models of cancer, TAMs regulate angiogenesis. For example in the PyMT model they have been shown to regulate the establishment of a high density vasculature – the so-called angiogenic switch - that is an important component of tumor progression (39). To determine whether there was any indication of changed vascular density in *Wnt7b* mutant tumors, we used a flow cytometry protocol to count CD31+, CD105+ vascular endothelial cells (VECs). This showed that at 22 weeks, there were reduced numbers of VECs in mutant tumors (Fig. 3A). To assess the density of functional vessels, we perfused tumor-bearing mice with Texas-red conjugated, lysine-fixable dextran (Fig. 3B, a highly reliable method for assessing vascular density as described previously (34)) and compared vessels per field (Fig. 3C) or branch-points per field (Fig. 3D) in stage-matched tumors. At premalignant tumor stages, both control and mutant tumors displayed the low vascular density typical of tumors that have not undergone the angiogenic switch (Fig. 3B–D). In early and late carcinomas of control mice, the vascular density was greatly increased (Fig. 3B–D) indicative of the angiogenic switch. By contrast, *Wnt7b* deleted mutant mice showed no significant change in the vascular density even though some tumors had progressed to early and late carcinomas (Fig. 3B–D). To assess vascular changes using another marker, we performed labeling with CD31 in 22-week control and mutant tumors. Quantification of CD31+ area (Fig. 3E) and CD31+ vessels (Fig. 3F) showed that by these measures too, mutant tumors showed reduced vascular density. These data show that TAM Wnt7b is required for the angiogenic switch.

VEGFA is a key stimulator of angiogenesis and a target gene of the Wnt/β-catenin pathway in some human tumors (40, 41). We assessed whether the failure of the angiogenic switch in *MMTV-PyMT* tumors might be associated with changes in *Vegfa* expression. In accordance with this hypothesis, the level of the *Vegfa* mRNA was significantly reduced in Wnt7b-deficient tumors at both the early and late carcinoma stages (Fig. 4A). Moreover, this was mirrored by a reduced level of Vegfa protein according to immunoblots (Fig. 4A, inset). When the Vegfa/actin optical density ratio of the control was normalized to 1.0±0.22 (n=3) mutant tumors showed a value of 0.65±0.07 (n=3, p=0.02). When CD31+ VECs were flow sorted from control and mutant tumors (Fig. S2A–C) and QPCR performed for *Vegfa* transcript, the mutants tumors showed reduced expression (Fig. S2D). This identifies tumor VECs as a likely source of *Vegfa* that is regulated by TAM Wnt7b. This also raises the possibility that Vegfa “private loop” signaling could function in the tumor context as it does in vascular system maintenance (42) and vascular development (43).

Flt1 (Vegfr1) is a naturally occurring inhibitor of Vegfa activity regulated in some contexts by Wnt signaling (44) and it was possible that increased expression could partly account for the angiogenic switch failure in *Wnt7b* mutant tumors. However, QPCR assessment of *Flt1*

transcript levels in control and mutant tumors of all stages did not reveal any significant changes (Fig. 4B). Vegfr2 is the major Vegfa signaling receptor (45). In some settings it has been shown that Vegfr3 can drive angiogenesis in absence of both Vegfa and Vegfr2 (46). To assess the expression of *Vegfr2* and *Vegfr3* in tumor VECs, we performed QPCR for these transcripts on flow-sorted cells from control and mutant tumors. This showed (Fig. S2D) that the transcript for both receptors were significantly up-regulated although the increase for Vegfr2 was, in absolute terms, modest. These data raise the possibility that Vegf receptor upregulation might partly compensate for reduced Vegfa ligand levels in the Wnt7b mutant tumor. Though it has been shown the Notch signaling in VECs can suppress expression of Vegfr2 and Vegfr3 (46), an assessment of the transcripts for the *Hey1* and *Dll4* genes that are the Notch pathway responsive (46) indicated no change (Fig. S2D). These data indicate that myeloid Wnt7b deletion results in modulation of several components of the Vegfa signaling pathway with the net result that angiogenic switching is deficient.

VECs are known to express the response machinery for the WNT/β-catenin pathway (25, 47, 48) and so it was possible that Wnt7b-dependent tumor progression was in part mediated by a direct effect. To assess the status of the WNT/β-catenin pathway in tumor VECs, we performed rapid flow-sorting of CD31+, CD105+ cells from 22 week tumors and performed QPCR for *Axin2, c-myc* and *CyclinD1*, three established WNT/β-catenin pathway target genes. As a control, we performed the same QPCR but from the whole tumor. This showed that while whole control and mutant tumors showed no significant change (Fig. 4C) the three WNT/β-catenin pathway target genes were all significantly reduced in VECs (Fig. 4D). These data identify VECs from the MMTV-PyMT tumor as WNT/β-catenin responsive. These data also raise the possibility that VECs respond directly to Wnt7b derived from TAMs.

To determine whether TAM WNT7b influenced tumor growth, we recorded gland volumes over the 6–22 week progression (Fig. 5A). Plotting these data on a log scale showed that though there were statistically significant differences at some time points between 6 and 18 weeks, in absolute terms, the differences were small and the growth curves nearly coincident (Fig. 5A). By contrast, there was a major divergence starting at 18 weeks in which control tumors increased in volume exponentially (Fig. 5A, gray trace) while the *Wnt7b*-deficient tumors plateaued in size (Fig. 5A, blue trace). In the control group, the tumor volume at 22 weeks was 650% of the 16-week tumor volume. In the mutant group, 22-week tumor volume was 170 % of the 16-week tumor volume. Tumors from the inguinal mammary glands were removed at 16 and 22 weeks and weighed. This showed that at both time-points, tumor mass in the mutant mice was significantly reduced compared with controls (Fig 5B, C). At 22 weeks, tumor weight in the mutant mice was 30% of tumor weight in the control mice. An assessment of proliferation using a Ki67 labeling index (Fig. 5D) showed that control and mutant early carcinomas showed indistinguishable levels of proliferation. In late carcinomas, control tumors showed a Ki67 labeling index that had nearly doubled (Fig. 5D). In contrast, mutant late carcinomas did not show elevated Ki67 labeling and remained at the level observed in early carcinomas (Fig. 5D). These data suggest that the size plateau observed in mutant tumors is at least partly explained by a failure of the proliferation rate to

elevate at late tumor stages. Combined, these data indicate that TAM WNT7b promotes tumor growth.

Prompted by the changes in tumor growth in the conditional mutant, we determined whether the stage of tumor progression was affected by TAM *Wnt7b* deletion. We assessed histological tumor progression on the basis of representative sections from 4 planes in each inguinal mammary gland at 16 and 22 weeks. This analysis was performed blind using criteria described previously (30). At 16 weeks, control and mutant tumors showed a similar distribution of stages (Fig. 5E). 44% of control and mutant tumors were hyperplasia or adenoma while 33% of control and 44% of mutant were early carcinomas. Only 22 and 11% of control and mutant tumors had progressed to late carcinomas at this time-point. At 22 weeks, about 90% of the control tumors were carcinomas and of these, the early-late carcinoma distribution was 30% and 60%. By contrast, myeloid *Wnt7b* deletion resulted in only 40% carcinomas with an equal distribution of early and late stages. Similarly, 12% of control tumors were hyperplasias or adenomas, but 56% of mutant tumors were at the same stage. Fisher's Exact Test showed that while the control tumors showed significant tumor progression between 16 and 22 weeks ($p=0.05$), the mutant tumors did not. Despite these observed delays in tumor progression in the Wnt7b-deficient mice, there were no noticeable differences in gross histology in stage-matched tumors, including the presence of necrotic regions, when conditional mutant and control tumors were compared. These results show that TAM WNT7b promotes malignant tumor progression.

The favored sites of metastasis in the MMTV-PyMT tumor model are lung and lymph node (30). Lungs from tumor bearing 22-week-old control mice showed metastases over a range of severity; typical examples of control and mutant lungs in whole mount (Fig. 6A and B) or section (Fig. 6C and D) are shown. To quantify the rate of metastasis in the control and *Wnt7b* conditional mutant, we isolated the lungs of 22-week-old mice and weighed them. The lungs of non-tumor bearing mice served as a negative control. Control, *MMTV-PyMT; Wnt7b*$^{-/tm2Amc}$ lungs were physically larger and weighed significantly more (Fig. 6E) than their control counterparts. Conditional deletion of *Wnt7b* prevented the increase in lung weight (Fig. 6E). Using QPCR amplification of the *MMTV-PyMT* transcript as an alternative measure of lung metastatic load also showed that mutant mice had reduced metastasis (Fig. 6F). A metastatic index calculated according to established and rigorous stereological methods (4) showed, like lung weight and PyMT transcript, that loss of *Wnt7b* from TAMs reduced the level of metastasis (Fig 6G).

Previous analysis has shown that in the MMTV-PyMT model, tumor cells and TAMs co-migrate out of the primary tumor (5). This co-migration includes intravasation and is driven by a paracrine feedback loop of TAM EGF and tumor cell CSF1 (5). This conclusion was based on several lines of evidence including intra-vital imaging of tumor cells and TAMs and an in vivo invasion assay in which we quantify the number of tumor cells and macrophages that migrate into a CSF1 or EGF-loaded microneedle inserted into the tumor (49). We used this in vivo invasion assay to determine the influence of TAM Wnt7b on tumor cell invasion. When the needles did not contain EGF, the number of cells entering the microneedles was small, as previously shown (Fig. 6H). However, when EGF was provided as a chemoattractant, many cells migrated in both the control and the Wnt7b conditional

mutant (Fig. 6H). The absence of TAM Wnt7b however, reduced the number of migrating cells by about two-fold (Fig. 6H). These data show, using several independent methods, that TAM WNT7b has an important role in promoting metastasis.

As a means of evaluating the findings in the mouse MMTV-PyMT model using human data, we returned to the Finak et al data set (38) that assessed gene expression in mammary carcinoma stroma, and performed gene expression correlation analysis with WNT7B. This has shown a limited but interesting set of correlations between stromal WNT7B some cell markers as well as chemokines and their receptors (Table 1). As might be expected, there was a significant positive correlation between WNT7B and the myeloid signaling factor CSF1 and between WNT7B and the myeloid marker CD209. Consistent with WNT7b-dependent angiogenic switching in the mouse model, there was also a significant positive correlation between WNT7B and the vascular marker CD31. Human stromal WNT7B is also significantly correlated with CCL3, CCL13, and CCR2. These correlations are consistent with existing analysis (50, 51) and may suggest that WNT7B shares a regulatory relationship with chemokines that influence tumor progression.

Discussion

In the current study, we have shown that human mammary carcinoma is strongly associated with over-expression of the WNT family ligand WNT7B in the tumor stroma and that isolated human breast carcinoma TAMs express WNT7B. Using experimental mice we have also shown that WNT7b has a key role in malignant progression of the MMTV-PyMT model of luminal breast cancer because it regulates the angiogenic switch, tumor progression, tumor growth, tumor cell invasion and metastasis. Using conditional inactivation of the *Wnt7b* gene with the myeloid restricted *Csf1r-icre* driver (28), we show that a critical source of Wnt7b is the TAM.

These data are consistent with prior work showing that TAMs can promote angiogenic switching (34) and that WNT7b can regulate angiogenesis and vascular remodeling in other settings including the developing neuroepithelium (26), the lung (33) and via macrophages, in the eye (25). TAMs in the PyMT model express Tie2 (Supplemental Fig. 1D–I) and it has also been shown that Tie2+ TAMs promote angiogenesis in models of spontaneous and orthotopic pancreatic tumors (7, 52). Importantly, TIE2 expression on the TAM is required for these cells to adhere to vessels, including in the PyMT model, and in the absence of TIE2, angiogenesis is inhibited (8). The observation that conditional *Wnt7b* inactivation results in reduced expression of several canonical WNT pathway target genes in VECs suggests that WNT7b directly stimulates the vasculature. Since WNT7B has a short range-of-action (25), it is likely that signaling is via cell-cell contact, a possibility consistent with the distribution of TIE2+ TAMs on the abluminal surfaces of tumor vasculature (30, 32, 49).

VEGFA is an established mediator of tumor angiogenesis (53). The current analysis shows that high *Vegfa* transcript and protein levels in the MMTV-PyMT tumor are dependent on Wnt7b. Furthermore, we show, using flow sorted cells, that tumor VECs are a source of *Vegfa* transcript and that myeloid Wnt7b normally upregulates this transcript. These data are consistent with the suggestion that tumor VECs can respond directly to myeloid Wnt7b. In

flow-sorted tumor VECs, we also observed an upregulation of the transcripts for Vegfr2 and Vegfr3 when Wnt7b was deleted from myeloid cells. We speculate that this change may partly compensate for the reduced level of Vegfa ligand. Though Vegfr2 and Vegfr3 transcripts can be suppressed by Notch signaling in some settings (46) the absence of any change in expression of the Notch responsive genes *Dll4* and *Hey1* (46) suggested that this was not the case in the VECs of the MMTV-PyMT tumor.

Vegfa gain-of-function in the PyMT model resulted in accelerated angiogeneic switching and accelerated tumor progression to malignancy in macrophage deficient mice (31). However, surprisingly, deletion of *Vegfa* from myeloid cells using *LysM-cre* resulted in increased tumor size and aggressiveness even though angiogenic switching was inhibited (54). In *LysM-cre; Vegfa*$^{fl/fl}$ mice, Vegfa levels were not changed overall but there was reduced Vegfa responsiveness. This contrasts with the current findings where conditional *Wnt7b* inactivation resulted in reduced tumor size and growth, a slower rate of tumor progression, a globally reduced level of *Vegfa* expression, and a loss of angiogenic switching. These differences probably reflect a function for WNT7b in directly eliciting responses from cells within the tumor and the likelihood that WNT7b-induced VEGFA expression is just one of these responses. Indeed, studies using the in vivo tumor cell-macrophage invasion assay show that in the absence of Wnt7b TAMs are less efficient at promoting tumor cell invasion. Furthermore, of great interest given the strong correlations between WNT7B expression and those of the chemokine signaling genes in stroma from human mammary carcinoma (Table 1) is the possibility that WNT7B regulates chemokine ligand and receptor expression and that these act as additional effectors of WNT7b-dependent tumor progression (50, 51, 55–57). It is notable that the major effect of conditional deletion of *Wnt7b* on MMTV-PyMT tumor progression is very similar to that observed when macrophages are depleted or ablated (4, 31, 34, 58) suggesting that WNT7b is required for the expression of many myeloid activities that promote tumor progression.

The loss of TAMs from the PyMT model resulted in a slowing in the rate of tumor progression particularly to malignancy (59). This is most likely due to the inhibition of the angiogenic switch as acceleration of this switch using a gain-of-function of CSF1 or VEGF either in wild type or macrophage deficient mice accelerated tumor progression (31, 34, 58, 60). In this study the loss of myeloid Wnt7b caused a similar phenotype to the ablation of TAMS with few tumors progressing to malignancy. On the genetic background used in the present studies this transition to malignancy was a little later than the 8–12 weeks reported for the original strain background (30) as even some wild type tumors had not progressed to malignancy by 16 weeks. Nevertheless, once the angiogenic switch was established and tumors progressed to malignancy, the wild type tumors accelerated in their growth as shown by a dramatic increase in mass accompanied by rapid proliferation as indicated by Ki67 staining. In contrast, the growth of WNT7b-deficient tumors growth plateaued with a reduced rate of proliferation (Ki67 positive cells) after 16 weeks of age presumably due to nutrient deficiency and deprivation of oxygen caused by an insufficient vascular network.

A key finding of this study is that *Wnt7b* inactivation in myeloid cells reduced pulmonary metastasis in the PyMT model. In this model, metastasis depends on tumor cells becoming malignant and escaping from the primary tumor into the hematogenous circulation. This

escape is a combination of enhanced invasiveness of tumor cells as well as the increased number of vascular targets. Loss of *Wnt7b* reduces the vascular density and has a direct effect on the ability of macrophages to promote tumor cell invasion in vivo. We suggest that this combination of changes reduces metastasis.

Csf1r-icre activity does, however, result in some deletion in cells of the acquired immune system (28) and confirmed in this study (data not shown). Nevertheless, in other studies the complete absence of B-cells in the MMTV-PyMT tumor does not change the rate of pulmonary metastasis (10) suggesting that the changes we observe are not likely to result from the inactivation of *Wnt7b* in B-cells. It has recently been shown that CD4+ T-cells promote pulmonary metastasis. This effect was through T-cell IL4 polarizing the function of TAMs to become pro-metastatic through their ability to induce tumor cell migration and invasion (10). However, in this study from Coussens' and co-workers, following depletion of T cells, angiogenesis was unimpaired. This indicates that Wnt7b derived from T cells is unimportant for angiogenesis. Furthermore, using the invasion assay we show directly that Wnt7b deficient macrophages are less able to stimulate tumor cell invasion in vivo. Consistent with these findings, our recent bioinformatics study showed that the TAMs that direct tumor cell intravasation and extravasation represent a unique subpopulation as defined by their gene expression signature with *Wnt7b* transcripts being highly represented in this signature (23). These data suggest a signaling relationship between the Wnt/β-catenin and IL4 pathways or alternatively, that each pathway independently supports a response required for pulmonary metastasis, perhaps at different stages of the process.

WNT7b expression also correlates with markers of poor prognosis such as lymph node positivity in human breast cancer (23) and through analysis of the Tissue Cancer Genome Atlas data sets it is highly up-regulated in breast (Fig 1A) and lung cancer (data not shown). Consistent with these data, *Wnt7b* expression up-regulation is a feature of the population of TAMs that promote angiogenesis and metastasis. The expression of WNT7b by TAMs from human tumors further suggests that therapeutic targeting of WNT7B responses might be beneficial in the treatment of some solid tumors. Because WNT7b responses promote many different aspects of tumor progression at multiple levels including three of the six recognized cancer hallmarks (39), WNT7B activity suppression is a uniquely promising therapeutic target likely to impact the rate of tumor metastasis, a key factor in patient survival.

Supplementary Material

Refer to Web version on PubMed Central for supplementary material.

Acknowledgments

We thank Paul Speeg for excellent technical assistance.

Financial Support: We acknowledge grant support from the NIH (PO1 CA100324, R01 EY021636-01 and 1R01CA131270 to R.A.L and J.W.P.), The Wellcome Trust (JWP) and from the Abrahamson Pediatric Eye Institute Endowment at Children's Hospital Medical Center of Cincinnati to R.A.L.

References

1. de Visser KE, Korets LV, Coussens LM. De novo carcinogenesis promoted by chronic inflammation is B lymphocyte dependent. Cancer Cell. 2005; 7:411–423. [PubMed: 15894262]
2. Andreu P, Johansson M, Affara NI, Pucci F, Tan T, Junankar S, Korets L, Lam J, Tawfik D, DeNardo DG, Naldini L, de Visser KE, De Palma M, Coussens LM. FcRgamma activation regulates inflammation-associated squamous carcinogenesis. Cancer Cell. 2010; 17:121–134. [PubMed: 20138013]
3. Lin EY, Nguyen AV, Russell RG, Pollard JW. Colony-stimulating factor 1 promotes progression of mammary tumors to malignancy. J Exp Med. 2001; 193:727–740. [PubMed: 11257139]
4. Qian B, Deng Y, Im JH, Muschel RJ, Zou Y, Li J, Lang RA, Pollard JW. A distinct macrophage population mediates metastatic breast cancer cell extravasation, establishment and growth. PLoS ONE. 2009; 4:e6562. [PubMed: 19668347]
5. Condeelis J, Pollard JW. Macrophages: obligate partners for tumor cell migration, invasion, and metastasis. Cell. 2006; 124:263–266. [PubMed: 16439202]
6. Qian BZ, Li J, Zhang H, Kitamura T, Zhang J, Campion LR, Kaiser EA, Snyder LA, Pollard JW. CCL2 recruits inflammatory monocytes to facilitate breast-tumour metastasis. Nature. 2011; 475:222–225. [PubMed: 21654748]
7. De Palma M, Venneri MA, Galli R, Sergi Sergi L, Politi LS, Sampaolesi M, Naldini L. Tie2 identifies a hematopoietic lineage of proangiogenic monocytes required for tumor vessel formation and a mesenchymal population of pericyte progenitors. Cancer Cell. 2005; 8:211–226. [PubMed: 16169466]
8. Coffelt SB, Chen YY, Muthana M, Welford AF, Tal AO, Scholz A, Plate KH, Reiss Y, Murdoch C, De Palma M, Lewis CE. Angiopoietin 2 stimulates TIE2-expressing monocytes to suppress T cell activation and to promote regulatory T cell expansion. J Immunol. 2011; 186:4183–4190. [PubMed: 21368233]
9. Ruffell B, Affara NI, Coussens LM. Differential macrophage programming in the tumor microenvironment. Trends in immunology. 2012; 33:119–126. [PubMed: 22277903]
10. DeNardo DG, Barreto JB, Andreu P, Vasquez L, Tawfik D, Kolhatkar N, Coussens LM. CD4(+) T cells regulate pulmonary metastasis of mammary carcinomas by enhancing protumor properties of macrophages. Cancer Cell. 2009; 16:91–102. [PubMed: 19647220]
11. Wang L, Yi T, Kortylewski M, Pardoll DM, Zeng D, Yu H. IL-17 can promote tumor growth through an IL-6-Stat3 signaling pathway. J Exp Med. 2009; 206:1457–1464. [PubMed: 19564351]
12. Logan CY, Nusse R. The Wnt signaling pathway in development and disease. Annu Rev Cell Dev Biol. 2004; 20:781–810. [PubMed: 15473860]
13. Garcia-Rostan G, Camp RL, Herrero A, Carcangiu ML, Rimm DL, Tallini G. Beta-catenin dysregulation in thyroid neoplasms: down-regulation, aberrant nuclear expression, and CTNNB1 exon 3 mutations are markers for aggressive tumor phenotypes and poor prognosis. Am J Pathol. 2001; 158:987–996. [PubMed: 11238046]
14. Pukkila MJ, Virtaniemi JA, Kumpulainen EJ, Pirinen RT, Johansson RT, Valtonen HJ, Juhola MT, Kosma VM. Nuclear beta catenin expression is related to unfavourable outcome in oropharyngeal and hypopharyngeal squamous cell carcinoma. J Clin Pathol. 2001; 54:42–47. [PubMed: 11271788]
15. Kinzler KW, Vogelstein B. Lessons from hereditary colorectal cancer. Cell. 1996; 87:159–170. [PubMed: 8861899]
16. Korinek V, Barker N, Morin PJ, van Wichen D, de Weger R, Kinzler KW, Vogelstein B, Clevers H. Constitutive transcriptional activation by a beta-catenin-Tcf complex in APC−/− colon carcinoma. Science. 1997; 275:1784–1787. [PubMed: 9065401]
17. Taniguchi K, Roberts LR, Aderca IN, Dong X, Qian C, Murphy LM, Nagorney DM, Burgart LJ, Roche PC, Smith DI, Ross JA, Liu W. Mutational spectrum of beta-catenin, AXIN1, and AXIN2 in hepatocellular carcinomas and hepatoblastomas. Oncogene. 2002; 21:4863–4871. [PubMed: 12101426]

18. Dahmen RP, Koch A, Denkhaus D, Tonn JC, Sorensen N, Berthold F, Behrens J, Birchmeier W, Wiestler OD, Pietsch T. Deletions of AXIN1, a component of the WNT/wingless pathway, in sporadic medulloblastomas. Cancer Res. 2001; 61:7039–7043. [PubMed: 11585731]
19. Nusse R, Varmus HE. Many tumors induced by the mouse mammary tumor virus contain a provirus integrated in the same region of the host genome. Cell. 1982; 31:99–109. [PubMed: 6297757]
20. Huguet EL, McMahon JA, McMahon AP, Bicknell R, Harris AL. Differential expression of human Wnt genes 2, 3, 4, and 7B in human breast cell lines and normal and disease states of human breast tissue. Cancer Res. 1994; 54:2615–2621. [PubMed: 8168088]
21. Bui TD, Zhang L, Rees MC, Bicknell R, Harris AL. Expression and hormone regulation of Wnt2, 3, 4, 5a, 7a, 7b and 10b in normal human endometrium and endometrial carcinoma. Br J Cancer. 1997; 75:1131–1136. [PubMed: 9099960]
22. Lindvall C, Bu W, Williams BO, Li Y. Wnt signaling, stem cells, and the cellular origin of breast cancer. Stem Cell Rev. 2007; 3:157–168. [PubMed: 17873348]
23. Ojalvo LS, Whittaker CA, Condeelis JS, Pollard JW. Gene expression analysis of macrophages that facilitate tumor invasion supports a role for Wnt-signaling in mediating their activity in primary mammary tumors. J Immunol. 2010; 184:702–712. [PubMed: 20018620]
24. Zheng D, Decker KF, Zhou T, Chen J, Qi Z, Jacobs K, Weilbaecher KN, Corey E, Long F, Jia L. Role of WNT7B-induced noncanonical pathway in advanced prostate cancer. Mol Cancer Res. 2013; 11:482–493. [PubMed: 23386686]
25. Lobov IB, Rao S, Carroll TJ, Vallance JE, Ito M, Ondr JK, Kurup S, Glass DA, Patel MS, Shu W, Morrisey EE, McMahon AP, Karsenty G, Lang RA. WNT7b mediates macrophage-induced programmed cell death in patterning of the vasculature. Nature. 2005; 437:417–421. [PubMed: 16163358]
26. Stenman JM, Rajagopal J, Carroll TJ, Ishibashi M, McMahon J, McMahon AP. Canonical Wnt signaling regulates organ-specific assembly and differentiation of CNS vasculature. Science. 2008; 322:1247–1250. [PubMed: 19023080]
27. Ojalvo LS, King W, Cox D, Pollard JW. High-density gene expression analysis of tumor-associated macrophages from mouse mammary tumors. Am J Pathol. 2009; 174:1048–1064. [PubMed: 19218341]
28. Deng L, Zhou JF, Sellers RS, Li JF, Nguyen AV, Wang Y, Orlofsky A, Liu Q, Hume DA, Pollard JW, Augenlicht L, Lin EY. A novel mouse model of inflammatory bowel disease links mammalian target of rapamycin-dependent hyperproliferation of colonic epithelium to inflammation-associated tumorigenesis. Am J Pathol. 2010; 176:952–967. [PubMed: 20042677]
29. Lin SL, Li B, Rao S, Yeo EJ, Hudson TE, Nowlin BT, Pei H, Chen L, Zheng JJ, Carroll TJ, Pollard JW, McMahon AP, Lang RA, Duffield JS. Macrophage Wnt7b is critical for kidney repair and regeneration. Proc Natl Acad Sci U S A. 2010; 107:4194–4199. [PubMed: 20160075]
30. Lin EY, Jones JG, Li P, Zhu L, Whitney KD, Muller WJ, Pollard JW. Progression to malignancy in the polyoma middle T oncoprotein mouse breast cancer model provides a reliable model for human diseases. Am J Pathol. 2003; 163:2113–2126. [PubMed: 14578209]
31. Lin EY, Li JF, Bricard G, Wang W, Deng Y, Sellers R, Porcelli SA, Pollard JW. Vascular endothelial growth factor restores delayed tumor progression in tumors depleted of macrophages. Mol Oncol. 2007; 1:288–302. [PubMed: 18509509]
32. Wyckoff J, Wang W, Lin EY, Wang Y, Pixley F, Stanley ER, Graf T, Pollard JW, Segall J, Condeelis J. A paracrine loop between tumor cells and macrophages is required for tumor cell migration in mammary tumors. Cancer Res. 2004; 64:7022–7029. [PubMed: 15466195]
33. Rajagopal J, Carroll TJ, Guseh JS, Bores SA, Blank LJ, Anderson WJ, Yu J, Zhou Q, McMahon AP, Melton DA. Wnt7b stimulates embryonic lung growth by coordinately increasing the replication of epithelium and mesenchyme. Development. 2008; 135:1625–1634. [PubMed: 18367557]
34. Lin EY, Li JF, Gnatovskiy L, Deng Y, Zhu L, Grzesik DA, Qian H, Xue XN, Pollard JW. Macrophages regulate the angiogenic switch in a mouse model of breast cancer. Cancer Res. 2006; 66:11238–11246. [PubMed: 17114237]

35. Yeo EJ, Chun YS, Cho YS, Kim J, Lee JC, Kim MS, Park JW. YC-1: a potential anticancer drug targeting hypoxia-inducible factor 1. J Natl Cancer Inst. 2003; 95:516–525. [PubMed: 12671019]
36. Hernandez L, Smirnova T, Kedrin D, Wyckoff J, Zhu L, Stanley ER, Cox D, Muller WJ, Pollard JW, Van Rooijen N, Segall JE. The EGF/CSF-1 paracrine invasion loop can be triggered by heregulin beta1 and CXCL12. Cancer Res. 2009; 69:3221–3227. [PubMed: 19293185]
37. Rhodes DR, Kalyana-Sundaram S, Mahavisno V, Varambally R, Yu J, Briggs BB, Barrette TR, Anstet MJ, Kincead-Beal C, Kulkarni P, Varambally S, Ghosh D, Chinnaiyan AM. Oncomine 3.0: genes, pathways, and networks in a collection of 18,000 cancer gene expression profiles. Neoplasia. 2007; 9:166–180. [PubMed: 17356713]
38. Finak G, Bertos N, Pepin F, Sadekova S, Souleimanova M, Zhao H, Chen H, Omeroglu G, Meterissian S, Omeroglu A, Hallett M, Park M. Stromal gene expression predicts clinical outcome in breast cancer. Nat Med. 2008; 14:518–527. [PubMed: 18438415]
39. Hanahan D, Weinberg RA. Hallmarks of cancer: the next generation. Cell. 2011; 144:646–674. [PubMed: 21376230]
40. Zhang X, Gaspard JP, Chung DC. Regulation of vascular endothelial growth factor by the Wnt and K-ras pathways in colonic neoplasia. Cancer Res. 2001; 61:6050–6054. [PubMed: 11507052]
41. Zhang B, Abreu JG, Zhou K, Chen Y, Hu Y, Zhou T, He X, Ma JX. Blocking the Wnt pathway, a unifying mechanism for an angiogenic inhibitor in the serine proteinase inhibitor family. Proc Natl Acad Sci U S A. 2010; 107:6900–6905. [PubMed: 20351274]
42. Lee S, Chen TT, Barber CL, Jordan MC, Murdock J, Desai S, Ferrara N, Nagy A, Roos KP, Iruela-Arispe ML. Autocrine VEGF signaling is required for vascular homeostasis. Cell. 2007; 130:691–703. [PubMed: 17719546]
43. Fan J, Ponferrada VG, Sato T, Vemaraju S, Fruttiger M, Gerhardt H, Ferrara N, Lang RA. Crim1 maintains retinal vascular stability during development by regulating endothelial cell Vegfa autocrine signaling. Development. 2014; 141:448–459. [PubMed: 24353059]
44. Stefater JA 3rd, Lewkowich I, Rao S, Mariggi G, Carpenter AC, Burr AR, Fan J, Ajima R, Molkentin JD, Williams BO, Wills-Karp M, Pollard JW, Yamaguchi T, Ferrara N, Gerhardt H, Lang RA. Regulation of angiogenesis by a non-canonical Wnt-Flt1 pathway in myeloid cells. Nature. 2011; 474:511–515. [PubMed: 21623369]
45. Ferrara N. VEGF-A: a critical regulator of blood vessel growth. European cytokine network. 2009; 20:158–163. [PubMed: 20167554]
46. Benedito R, Rocha SF, Woeste M, Zamykal M, Radtke F, Casanovas O, Duarte A, Pytowski B, Adams RH. Notch-dependent VEGFR3 upregulation allows angiogenesis without VEGF-VEGFR2 signalling. Nature. 2012; 484:110–114. [PubMed: 22426001]
47. Goodwin AM, D'Amore PA. Wnt signaling in the vasculature. Angiogenesis. 2002; 5:1–9. [PubMed: 12549854]
48. Franco CA, Liebner S, Gerhardt H. Vascular morphogenesis: a Wnt for every vessel? Curr Opin Genet Dev. 2009; 19:476–483. [PubMed: 19864126]
49. Wyckoff JB, Wang Y, Lin EY, Li JF, Goswami S, Stanley ER, Segall JE, Pollard JW, Condeelis J. Direct visualization of macrophage-assisted tumor cell intravasation in mammary tumors. Cancer Res. 2007; 67:2649–2656. [PubMed: 17363585]
50. Ren G, Zhao X, Wang Y, Zhang X, Chen X, Xu C, Yuan ZR, Roberts AI, Zhang L, Zheng B, Wen T, Han Y, Rabson AB, Tischfield JA, Shao C, Shi Y. CCR2-dependent recruitment of macrophages by tumor-educated mesenchymal stromal cells promotes tumor development and is mimicked by TNFalpha. Cell stem cell. 2012; 11:812–824. [PubMed: 23168163]
51. Fang WB, Jokar I, Zou A, Lambert D, Dendukuri P, Cheng N. CCL2/CCR2 chemokine signaling coordinates survival and motility of breast cancer cells through Smad3 protein- and p42/44 mitogen-activated protein kinase (MAPK)-dependent mechanisms. J Biol Chem. 2012; 287:36593–36608. [PubMed: 22927430]
52. De Palma M, Venneri MA, Roca C, Naldini L. Targeting exogenous genes to tumor angiogenesis by transplantation of genetically modified hematopoietic stem cells. Nat Med. 2003; 9:789–795. [PubMed: 12740570]

53. Ferrara N, Hillan KJ, Gerber HP, Novotny W. Discovery and development of bevacizumab, an anti-VEGF antibody for treating cancer. Nat Rev Drug Discov. 2004; 3:391–400. [PubMed: 15136787]
54. Stockmann C, Doedens A, Weidemann A, Zhang N, Takeda N, Greenberg JI, Cheresh DA, Johnson RS. Deletion of vascular endothelial growth factor in myeloid cells accelerates tumorigenesis. Nature. 2008; 456:814–818. [PubMed: 18997773]
55. Strieter RM, Belperio JA, Burdick MD, Sharma S, Dubinett SM, Keane MP. CXC chemokines: angiogenesis, immunoangiostasis, and metastases in lung cancer. Ann N Y Acad Sci. 2004; 1028:351–360. [PubMed: 15650260]
56. Karnoub AE, Weinberg RA. Chemokine networks and breast cancer metastasis. Breast disease. 2006; 26:75–85. [PubMed: 17473367]
57. Zlotnik A, Burkhardt AM, Homey B. Homeostatic chemokine receptors and organ-specific metastasis. Nat Rev Immunol. 2011; 11:597–606. [PubMed: 21866172]
58. Lin EY, Pollard JW. Tumor-associated macrophages press the angiogenic switch in breast cancer. Cancer Res. 2007; 67:5064–5066. [PubMed: 17545580]
59. Lin EY, Pollard JW. Macrophages: modulators of breast cancer progression. Novartis Found Symp. 2004; 256:158–168. discussion 168–172, 259–169. [PubMed: 15027489]
60. Lin EY, Li JF, Bricard G, Wang W, Deng Y, Sellers R, Porcelli SA, Pollard JW. VEGF Restores Delayed Tumor Progression in Tumors Depleted of Macrophages. Mol Oncol. 2007; 1:288–302. [PubMed: 18509509]

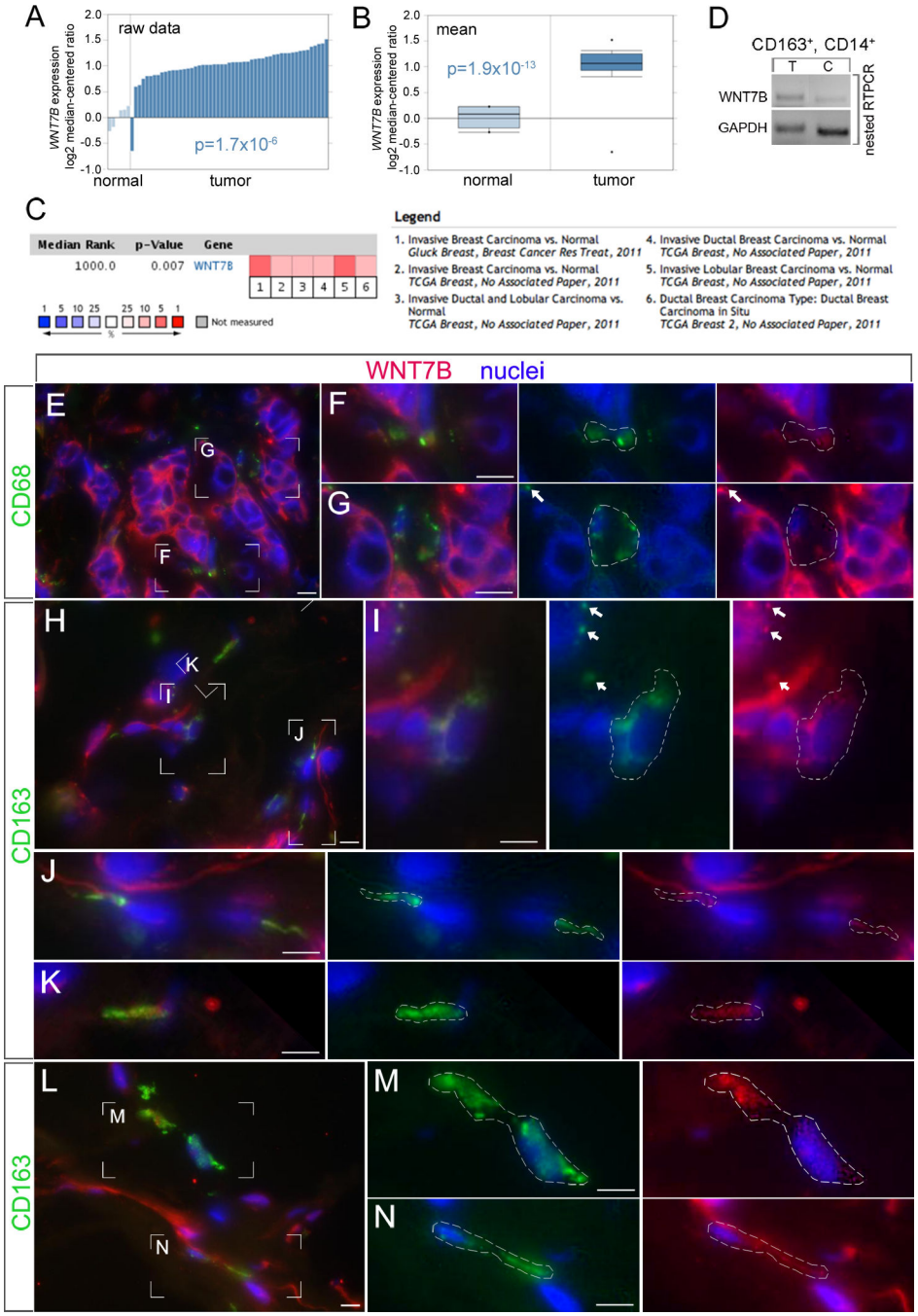

Fig 1. WNT7B expression in human mammary tumors

WNT7B expression (as log2 median centered ratio) for mammary gland, normal and tumor stroma, shown either as raw data (A) or as the mean (B). In the chart showing the mean, the dots indicate the extreme data values. Significance as labeled. (C) Meta-analysis of recent gene expression profiling for WNT7B where the colored squares indicate the median rank for WNT7B across each analysis. WNT7B ranks in the top 5–10% in all 6 analyses. (D) End-point RT-PCR for WNT7B in flow-sorted CD45+, CD11b+, CD163+, CD14+ TAMs from human mammary carcinoma (T) and adjacent normal tissue (C). (E–N)

Immunoreactivity in cryosections of human mammary carcinoma for WNT7B (red) and the TAM markers CD68 (green) or CD163 (green) as labeled. Images at 600× magnification (E, H, L) show boxed regions (F, G, I–K, M, N) that are digitally magnified in the adjacent panels. Magnified panels are in sets that show all the color channels or just the TAM marker (green) with nuclei (blue) or WNT7B (red) with nuclei (blue). In the magnified panels, a dashed line or a white arrow indicates the green-labeled region identifying a TAM. Adjacent, these same regions are indicated in images where only the WNT7B labeling (red) is shown. In all cases, WNT7B immunoreactivity is associated with TAMs and their processes. The tumor cells are also strongly immunoreactive with the WNT7B antibody. The white scale bars are 10 μm.

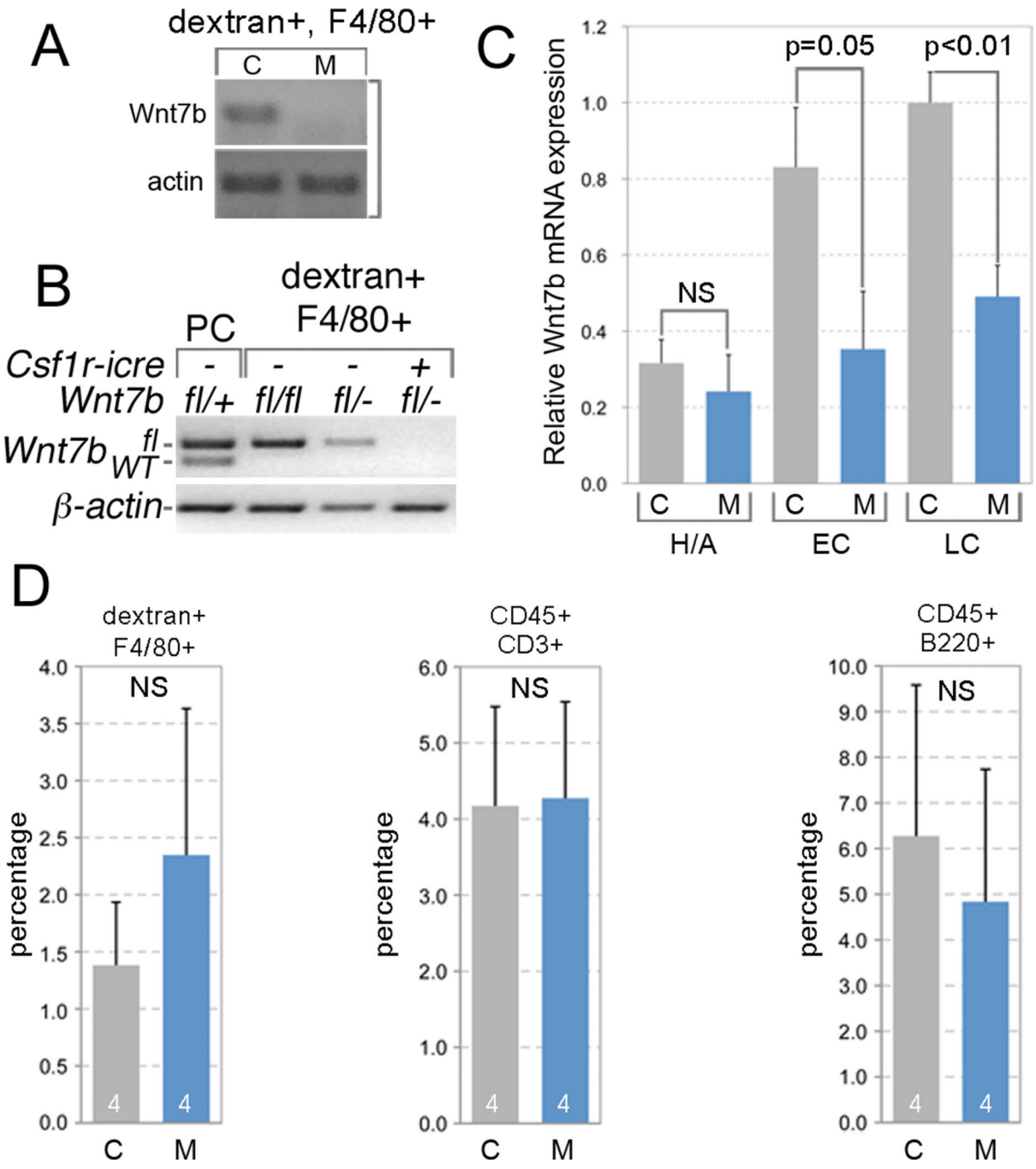

Fig. 2. *Wnt7b* expression and deletion in the MMTV-PyMT model

(A) End-point RT-PCR for Wnt7b from in flow-sorted dextran+, F4/80+ mouse macrophages from *Wnt7b*$^{tm2Amc/-}$ (control, C) and *Wnt7b*$^{tm2Amc/-}$*; Csf1r-icre* (mutant, M) MMTV-PyMT tumors. (B) Genotyping PCR on peritoneal cells (PC) or in flow-sorted dextran+, F4/80+ macrophages from MMTV-PyMT tumors of the indicated genotypes. The PCR primers used do not amplify a product from the recombined *Wnt7b*^{tm2Amc} allele. (C) Relative *Wnt7b* mRNA expression in control (C) and mutant (M) *MMTV-PyMT* mammary tumors at premalignant (Hyperplasia and Adenoma, H/A), or malignant (early carcinoma,

EC, and late carcinoma, LC) stages. Error bars are SEM. (D) Percentage of marker positive cells in control (*MMTV-PyMT; Wnt7b*$^{tm2Amc/-}$, C) and mutant (*MMTV-PyMT; Wnt7b*$^{tm2Amc/-}$*; Csf1r-iCre*, M) tumors combined from the 20–22 week range. Error bars are SEM.

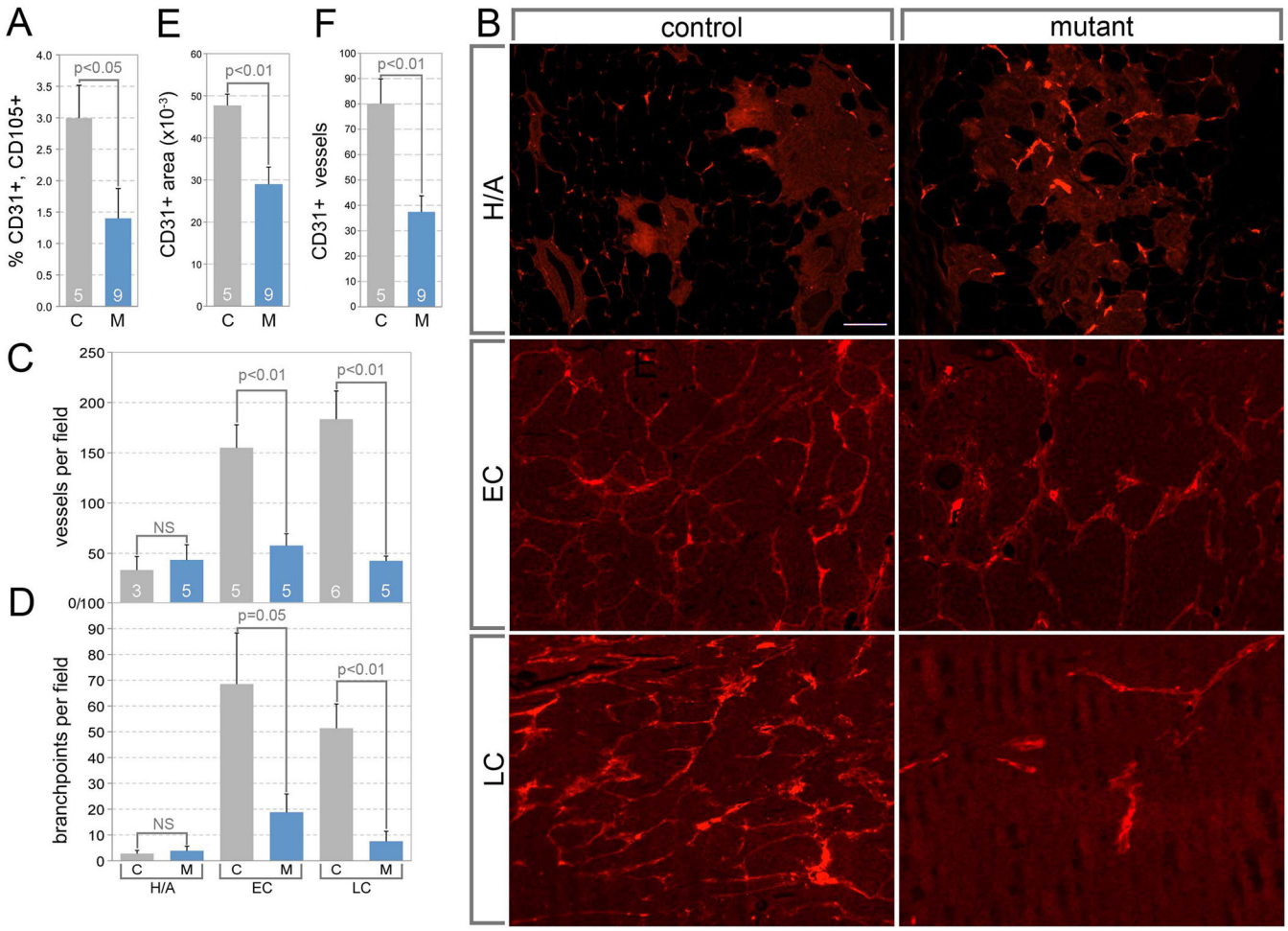

Fig 3. The angiogenic switch is suppressed in the absence of TAM Wnt7b

(A) Percentage of CD31+, CD105+ vascular endothelial cells in control and mutant tumors combined from the 20–22 week range. (B) Representative images of Texas Red dextran perfused blood vessels in PyMT mammary tumors at premalignant (Hyperplasia and Adenoma, H/A), or malignant (early carcinoma, EC, and late carcinoma, LC) stages. The scale bar in (B), H/A, control is 100 μm and applies to all panels. (C, D) Quantification of dextran labeled vessels for a given tumor stage using either vessels per field (C) or branch-points per field (D). (E, F) Quantification of CD31 labeling in control (C) and mutant (M) late carcinomas shown either as CD31+ area (E) or CD31+ vessels (F). For (A and C–F) sample number is shown at base of histogram bar. Error bars are SEM.

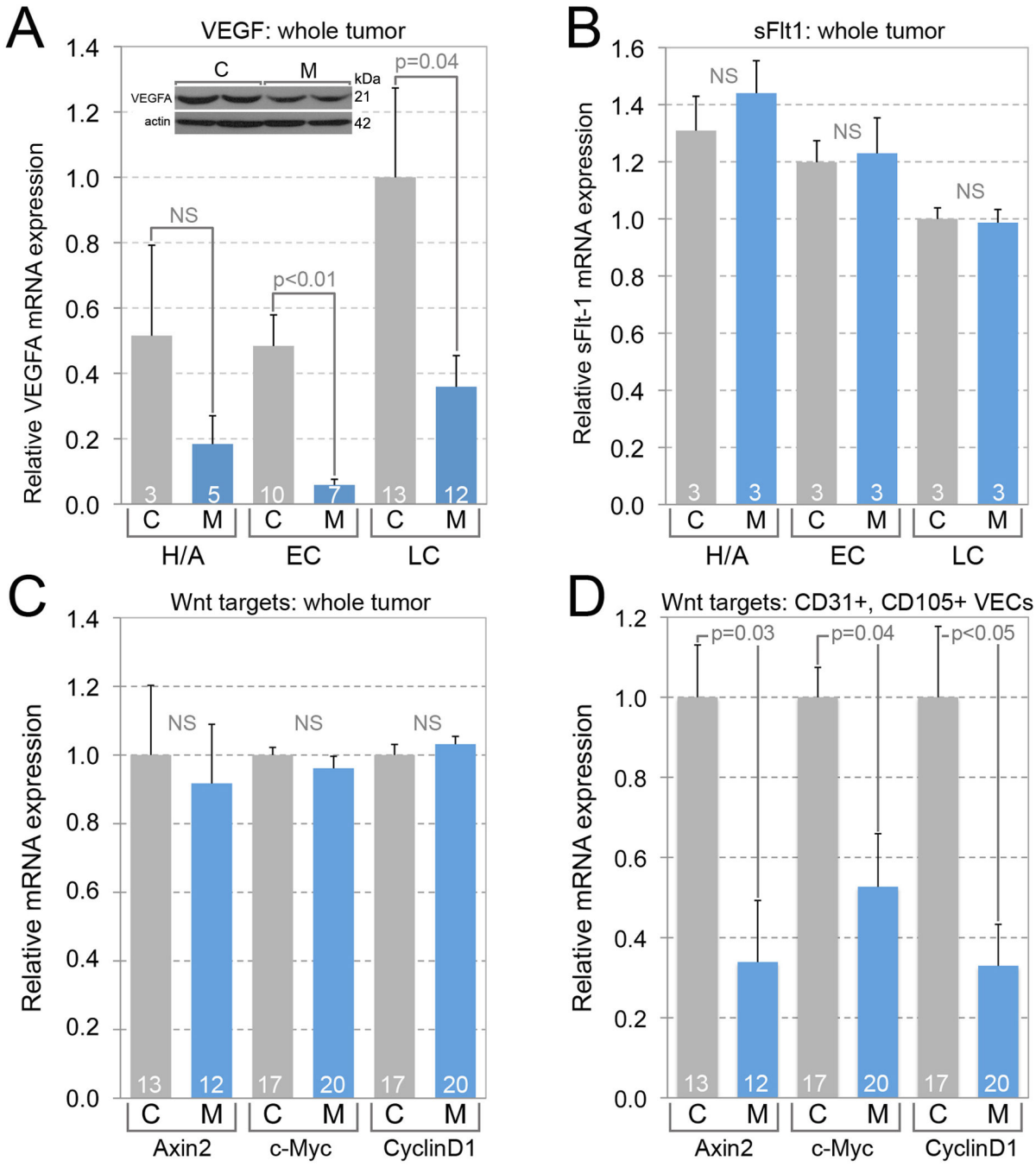

Fig 4. The expression of Vegfa is reduced by the deletion of tumor stroma cell Wnt7b

(A) Relative *Vegfa* mRNA expression in control (C) and mutant (M) MMTV-PyMT tumors at H/A, EC and LC stages. Inset: Immunoblotting for VEGFA and actin control and mutant MMTV-PyMT tumor lysates. (B) Relative *sFlt-1* mRNA level in control and mutant MMTV-PyMT tumors at H/A, EC and LC stages. (C, D) Relative expression of *Axin2*, *c-Myc*, and *CyclinD1* in control and mutant whole tumor (C) and CD31+, CD105+ blood vascular endothelial cells (D). Sample number is shown at the base of each histogram bar. Error bars are SEM.

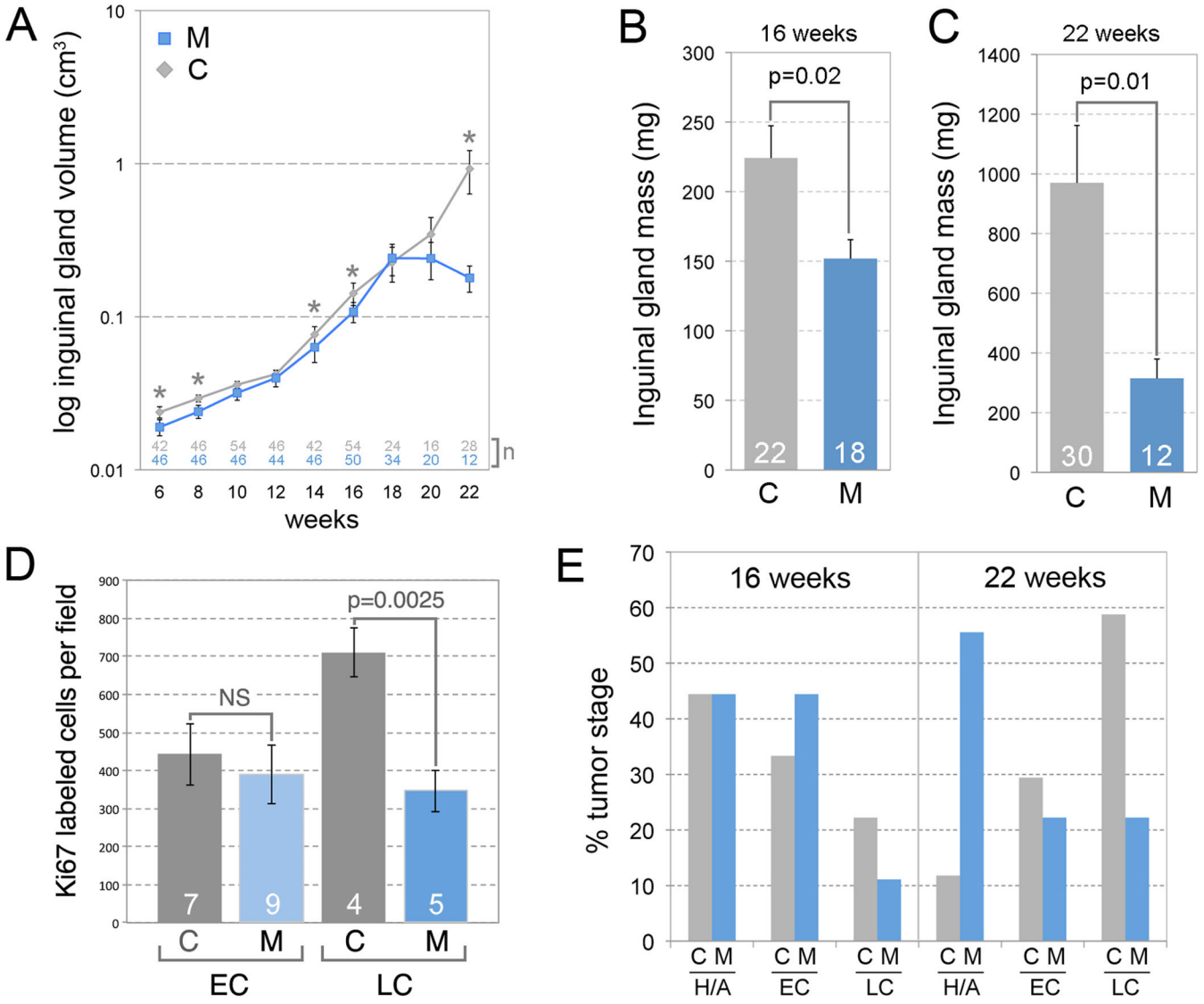

Fig. 5. TAM *Wnt7b* deletion suppresses tumor volume, mass and progression

(A) Control and mutant inguinal gland volume from 6 weeks to 22 weeks. (B, C) Inguinal gland mass at 16 (B) and 22 (C) weeks. For (B, C) sample number is shown at the base of the chart. Error bars are SEM. (D) Ki67 labeled cells per field for control (*MMTV-PyMT; Wnt7b*$^{tm2Amc/-}$, C) and mutant (*MMTV-PyMT; Wnt7b*$^{tm2Amc/-}$*; Csf1r-iCre*, M) early carcinomas (EC) and late carcinomas (LC). P values as labeled, error bars are SEM. (E) Distribution of the stage of progression for control (C) and mutant (M) MMTV-PyMT mammary tumors at 16 weeks (for control, C, n=18, for mutant, M, n=18) and 22 weeks (for C, n=17, for M, n=9). Hyperplasia and adenoma: H/A, early carcinoma: EC, and late carcinoma: LC.

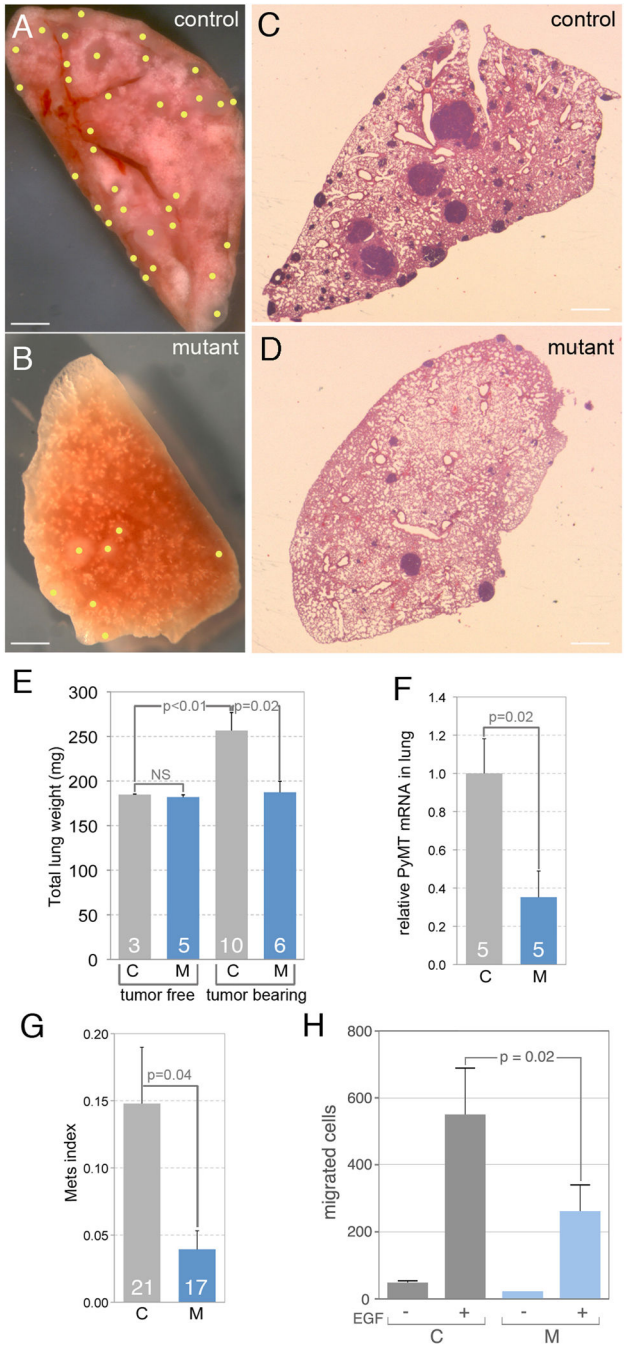

Fig 6. Metastasis is reduced in the absence of tumor stroma cell WNT7b

(A–D) Representative images of metastasized lung in control (A, C) and mutant (B, D) mice in whole mount (A, B) and in section (C, D) at 22 weeks. Scale bars in (A–D) are 180 μm. (A, B) Obvious surface metastases in whole mount lungs are marked with yellow dots. (C, D) In lung sections, metastases appear as dense purple regions. (E) Quantification of total lung weight in control and mutant, tumor free and tumor bearing mice at 22 weeks. (F) Relative PyMT mRNA expression in control and mutant lung at 22 weeks. (G) The lung metastasis index for control and mutant mice at 22 weeks. Sample number is shown at the

base of each histogram bar in (E–G). (H) Quantification of the number of cells that migrate into micro-needles placed in either control (*MMTV-PyMT; Wnt7b*$^{tm2Amc/-}$, C) or mutant (*MMTV-PyMT; Wnt7b*$^{tm2Amc/-}$*; Csf1r-iCre*, M) tumors. The micro-needles were loaded with either vehicle (−) or EGF (+) as labeled. These data show that the absence of TAM Wnt7b significantly reduced the number of cells that migrate into the needle under the influence of EGF. Error bars for all charts are SEM.

Table 1

Expression correlations with WNT7B in the stroma of human mammary carcinoma

Marker/chemokine	R factor	P value
CSF1	0.091	0.0311
CD209	0.211	0.0007
CD31	0.268	0.0001
CCL3	0.087	0.0353
CCL13	0.139	0.0070
CCR2	0.158	0.0039

The expression level of IL4, IL6, IL10, TGFβ, CSF1R, CD14, CD11b, CD163, CCL2, CCL4, CCL5, CCL7, CCL8, CCL19, CXCL2, CXCL14, CXCL16, CCR1, and CCR5 were not significantly correlated with expression level of WNT7B